Thermal excitation of heavy nuclei with 5-15 GeV/c antiproton, proton and pion beams

L. Beaulieu [a] K. Kwiatkowski [a,1] W.-c. Hsi [a] T. Lefort [a]
L. Pienkowski [b] R.G. Korteling [c] G. Wang [a,2] B. Back [d]
D.S. Bracken [a,1] H. Breuer [e] E. Cornell [a,3] F. Gimeno-Nogues [f]
D.S. Ginger [a,4] S. Gushue [g] M.J. Huang [h] R. Laforest [f,5]
W.G. Lynch [h] E. Martin [f] K.B. Morley [i] L.P. Remsberg [g]
D. Rowland [f] E. Ramakrishnan [f] A. Ruangma [f] M.B. Tsang [h]
V.E. Viola [a] E. Winchester [f] H. Xi [h] S.J. Yennello [f]

[a] *Department of Chemistry and IUCF, Indiana University, Bloomington, IN 47405*

[b] *Heavy Ion Laboratory, Warsaw University, Warsaw Poland*

[c] *Department of Chemistry, Simon Fraser University, Burnaby, BC, Canada V5A IS6*

[d] *Physics Division, Argonne National Laboratory, Argonne IL 60439*

[e] *Department of Physics, University of Maryland, College Park, MD 20740*

[f] *Department of Chemistry & Cyclotron Laboratory, Texas A&M University, College Station, TX 77843*

[g] *Chemistry Department, Brookhaven National Laboratory, Upton, NY 11973*

[h] *Department of Physics and NSCL, Michigan State University, East Lansing, MI 48824*

[i] *Los Alamos National Laboratory, Los Alamos, NM 87545*

Abstract

Excitation-energy distributions have been derived from measurements of 5.0-14.6 GeV/c antiproton, proton and pion reactions with ^{197}Au target nuclei, using the ISiS 4π detector array. The maximum probability for producing high excitation-energy events is found for the 8 GeV/c antiproton beam relative to other hadrons, ^{3}He and $\bar{p}$ beams from LEAR. For protons and pions, the excitation-energy distributions are nearly independent of hadron type and beam momentum above about 8 GeV/c. The excitation energy enhancement for $\bar{p}$ beams and the saturation effect are qualitatively consistent with intranuclear cascade code predictions. For all systems studied, maximum cluster sizes are observed for residues with E*/A $\sim$ 6 MeV.

*PACS:*25.70.Pq,25.43.+t,25.80.Hp

Much effort in nuclear physics has been devoted to the study of the formation of multiple complex fragments ($3 \leq Z \leq 16$), or multifragmentation, and its possible link to the nuclear liquid-gas phase transition [1]. In particular, the strong interest created by the measurement of a latent heat by Pochodzalla *et al.* [2], which would signal a first order phase transition. However, in many cases multifragmentation of heavy nuclei is not only driven by the its thermal and Coulomb properties, but also by collective (dynamical) properties of the chaotic systems formed in energetic projectile-target interactions.

The thermal features of the breakup process are isolated most transparently in reactions induced by hadron and light-ion beams at energies in excess of 2 GeV[3–5]. Transport calculations predict that such beams heat nuclei rapidly, $\tau \leq$ 30-40 fm/c, at the same time producing little compression, low average angular momentum and minimal shape distortions[6,7]. While excitation energy deposition E^* in GeV hadron-induced reactions is significantly less than the total available energy[3,4], transport calculations indicate that residues can be created in such collisions with E^* values well in excess of the multifragmentation threshold, $E^*/A \sim 5$ MeV[8–10]. The objective of the present study is to investigate the relative effectiveness of various hadron beams and momenta for producing E* values in excess of ~ 5 MeV/A, thereby identifying the optimum system for studies of thermal multifragmentation and underlying phenomena e.g. the liquid-gas phase transition.

In Fig. 1, excitation-energy predictions of the Toneev[11] intranuclear cascade calculation (INC) are shown. Here the average excitation energy imparted to a ^{197}Au nucleus by proton, π^- and antiproton beams is plotted as a function of beam momentum. For p and π^- beams, the $\langle E^* \rangle$ values are predicted to be nearly identical; above about 8 GeV/c there is little dependence on beam momentum. These features have been verified qualitatively in charged-particle multiplicity studies by Hsi *et al.*[12] and in earlier inclusive studies by Porile[13]. However, the antiproton predictions exhibit a significant increase in average excitation energy. This enhancement derives from reabsorption of some fraction of the annihilation pions ($< n_\pi > \sim 5$), which complements the internal heating caused by the cascade of hadron-hadron collisions and Δ resonance excitations[6,11,14]. From the point of view of multifragmentation, this greatly enhances the probability for forming residues excited above the multifragmentation threshold, as shown in the inset of Fig. 1, where E^*

[1] Present address: Los Alamos National Laboratory, Los Alamos, NM 87545
[2] Present address: Epsilon, Inc., Dallas, TX 75240
[3] Present address: Lawrence Berkeley Laboratory, Berkeley, CA 94720
[4] Cambridge University, Cambridge, U.K.
[5] Barnes Hospital, Washington University, St. Louis, MO 63130

distributions for 8 GeV/c π^- and $\bar{p}$ are compared.

In this letter we present results for excitation-energy distributions derived from bombardments of ^{197}Au nuclei with 5.0-14.6 GeV/c hadron beams. Exclusive charged-particle multiplicities and energy spectra were measured at the Brookhaven AGS accelerator with the Indiana Silicon Sphere, a 4π detector array with 162 gas-ion-chamber/silicon/CsI telescopes[15]. Two experiments were performed. The first used untagged negative beams (largely π^-) at 5.0, 8.2, and 9.2 GeV/c and positive beams (primarily protons) at 6.2, 10.2, 12.8 and 14.6 GeV/c. The second was performed with a tagged 8.0 GeV/c negative beam, which provided simultaneous measurement of the π^- (98%) and $\bar{p}$ (1%) reactions. The results at 8 GeV/c for the two π^- experiments are found to be identical within error bars. Further experimental details can be found in[12,15,16]. As part of our analysis, we have also compared with data from the 4.8 GeV ^{3}He + ^{197}Au reaction[4] at LNS Saclay and the 1.2 GeV/c $\bar{p}$ + ^{197}Au reaction from LEAR[3].

In the experiments reported here, calculation of the excited residue charge and mass was made by subtracting fast cascade particles from the target charge and mass using the same procedure as in ref [4]. Excitation-energy reconstruction was performed for each event by calorimetry according to the following prescription:

$$E^* = \sum_{i=1}^{M_c} K_i + M_n < K_n > + Q + E_\gamma. \quad (1)$$

Here, K_i is the kinetic energy of each charged particle in an event of multiplicity M_c, M_n and $\langle K_n \rangle$ are the multiplicity and average kinetic energy of neutrons, Q is the mass difference of the reconstructed event, and E_γ is a small term to account for gamma de-excitation of the residual nucleus and excited fragments. This procedure is similar to those employed in[4,16,17,2,18–20] and a full paper on the dependence of E^* values on the various assumptions of the reconstruction and the effects of fluctuations is in preparation.

For the present measurements the two most sensitive parameters of the reconstruction procedure involve the assumption concerning $\langle K_n \rangle$ and the definition of the energy range for thermal-like particles. Since neutrons are not measured in ISiS, we use the neutron-charged particle correlations reported for LEAR data by Goldenbaum *et al.*[3]. This correlation is in good agreement with similar results from heavy-ion reactions[21] and model simulations[8,9,22]. However, systematic uncertainties arise when the kinetic energies are assigned to the neutrons. The neutron average kinetic energies were taken from the predicted correlation between $\langle K_n \rangle$ and E*/A by SMM[8]. Then Eq. 1 is iterated to obtain self-consistency. Similar values are obtained from an iterative procedure using $E^* = aT^2$ and an initial value of $\langle K_n \rangle = T$. Comparison between unfiltered and filtered simulations with SMM[8] and the evaporation code SI-

MON [22] both show that the use of $3T/2$ (initial $\langle K_n \rangle = 3T/2$) overpredicts the values of $\langle K_n \rangle$ by as much as 30% at high E^*, resulting in an overestimation of E^* of about 10-12% ($\sim$ 20% for initial $\langle K_n \rangle$=$2T$).

Thermal-like charged particles are defined by the spectral shapes, from which an upper cutoff of 30 MeV for H and $9Z + 40$ MeV for heavier fragments was assigned [4,5]. Our definition of E^* is a conservative one; for example, with the expanded charged particle acceptance ($E/A < 30$ MeV) of Hauger *et al.*[20], we obtain E^* values about 25% higher than reported here.

Finally, the stability of the E^* reconstruction procedure has been tested using SMM and SIMON. Both models give a strong linear correlation between the unfiltered and filtered E^*. The average values are recovered by the method with deviation not larger than $\pm$10% over the useful range of the data (E^*/A=2-9 MeV). A detailed comparison will be presented in a long paper. However, the approach taken above should be viewed as a conservative one, as should the E^* distributions.

In Figure 2 we show the reconstructed probability distributions for excitation energy and residue mass for the range of systems studied in this work, where $\sum_i P(E_i^*) = 1$. Values of E^* below 250 MeV become highly uncertain due to the dominance of neutron emission (unmeasured in ISiS) at low excitation energies and the suppression of $M_c \leq 2$ events by the ISiS trigger. Data for 6.2 GeV/c and 12.8 GeV/c protons (not shown) are similar to other proton and pion data in Figs. 2-5. Fig.2 demonstrates that the largest population of high excitation energy events is achieved with the 8.0 GeV/c $\bar{p}$ beam and the lowest with the 5.0 GeV/c π^- beam. The 12.8 GeV/c proton distribution is slightly higher than for 14.6 GeV/c p, while that for the 6.2 GeV/c protons is slightly lower than the 8 GeV/c π^-. Thus, the data and the INC predictions of Fig. 1 are in qualititive agreement. Quantitatively, however, the INC calculations predict E^* distributions that extend significantly beyond the data, as discussed in[16].

The residue mass distributions show a somewhat different pattern. In this case the 14.6 GeV/c proton beam produces the lightest residues and the 5.0 GeV/c π^- the heaviest. This mass dependence can be understood as a consequence of the fast cascade, which produces an increasing number of fast knockout particles as the beam momentum increases, and also leads to a density-depleted residue[6,7]. This process produces the saturation in average excitation energy shown in the INC calculations of Fig.1 and the data in Fig.2. That is, the increase in total available beam energy for E^* deposition is counterbalanced by loss of energy due to mass loss ΔA during the fast cascade. This mass loss, derived from the data, is shown in the top panel of Fig.3 as a function of deposited excitation energy.

The relative effectiveness of various beams in depositing high excitation energies is shown in the bottom panel of Fig. 3 and summarized in Table 1. Included here are comparable data from the 4.8 GeV ^{3}He + ^{197}Au reaction[4] and the 1.2 GeV $\bar{p}$ + ^{197}Au reaction[3]. In order to emphasize the probability for forming highly excited systems, we examine the ratio of total events with E^* greater than a given value to that for events with $E^* \geq 400$ MeV. At E^*=400 MeV, the event reconstruction should provide the greatest self-consistency among the data sets.

Figure 3 and Table 1 confirm that the 8.0 GeV/c antiproton beam produces a significant enhancement of high excitation energy events, particularly in the multifragmentation regime above 800-1000 MeV. In Table 1, the yield of events with excitation energy above the multifragmentation threshold for Au-like nuclei (a range that spans 800-1000 MeV or about 5 MeV/nucleon) is listed, compared to total events above E^* >400 MeV (E^*/A >2 MeV). The enhancement for the 8 GeV/c $\bar{p}$ beam is approximately 25% greater than the next most effective beam, 12.8 GeV/c protons. Relative to the $\bar{p}$ studies with 2.1 GeV/c $\bar{p}$ at LEAR [3], where negligible multifragmentation yield was observed, the probabilities for high E^* events at 8 GeV/c are over an order of magnitude greater. In this regard, we note that for the 1.8 GeV ^{3}He + ^{197}Au system [23], for which the charged-particle multiplicity data are very similar to those with LEAR beams [24], the total cross section for events with four or more Z $\geq$ 3 fragments is only 3.5 mb. At the higher energy of 4.8 GeV, this cross section has grown to 83 mb. Thus, when account is made for the rapid growth of multifragmentation cross section with increasing beam momentum, the ISiS results and those of Ref. [3] appear to be self-consistent.

In Fig. 4 the excitation energy distributions are plotted as a function of E^*/A of the residue. We note here, as well as in Fig 5, that events with $E^*/A \geq$ 9 MeV comprise less than 1% of the data set. The same general features persist as in Fig. 3, except in this case the 14.6 GeV/c proton beam yields comparable probabilities in the region beyond about $E^*/A > 9$ MeV. Two factors account for this. First, the average residue mass is lighter for reactions at this momentum, as shown in Fig. 2. Second, the number of events obtained with the 8.0 GeV/c $\bar{p}$ beam ($\sim$ 25,000) were about two orders of magnitude lower than for the other beams, creating larger statistical uncertainties at the extremes.

Finally, in Fig. 5 we examine the dependence of the fragment size distributions on E*/A, of relevance to discussions of critical phenomena and a nuclear liquid-gas phase transition[13,20]. The top panel shows the number of observed IMFs per residue nucleon and the corresponding filter-corrected value as a function of E^*/A for the various reactions. This ratio is nearly identical for all systems, increasing systematically with increasing E^*/A up to 9 MeV and then becoming roughly constant thereafter. The same uniformity is ob-

served in the fragment charge distributions, shown in the lower panel of Fig. 5, where the parameter τ from power-law fits to the charge distributions are plotted as a function of E^*/A. Values of τ decrease steadily as the system is heated i.e. the probability for forming larger fragments increases. A minimum is reached at $\tau \sim 2$ near $E^*/A \sim 6$ MeV, followed by a slight increase (smaller fragments). This signifies that maximum cluster sizes are obtained very near the multifragmentation threshold. Thereafter, additional excitation appears to produce a hotter environment, leading to an increased yield of lighter particles and clusters.

In summary, the heat content (E^*) of equilibrium-like heavy residues formed in 5-15 GeV/c hadron-induced reactions has been investigated. The antiproton beam is found to be most effective in creating highly excited residues, in qualitative agreement with INC predictions. Relative to the threshold for multifragmentation in such systems ($E^* \sim$ 800-1000 MeV), the enhancement of high excitation energy events with antiprotons is at least 25-35% greater than other hadrons and over an order of magnitude greater than antiprotons from LEAR. Above momenta of about 8 GeV/c the probability for E^* deposition with hadron beams is nearly independent of hadron type or beam momentum, again consistent with INC calculations. The observed average number of IMF per residue nucleon and the power-law fits to the charge distributions show a universal behavior as a function of E^*/A. This independence of the final multifragmentation state on collision dynamics suggests equilibrium-like behavior in the breakup of the hot residues [25,26]. Therefore hadron, especially antiprotons around 6-8 GeV/c and pions or protons above 10-12 GeV/c, are very well suited to study thermal multifragmentation. For a given beam momentum, they provide a wide range of thermal energy (E^*/A), which is an essential quantity for investigating latent heat in nuclear matter and related properties.

Acknowledgements

The authors thank J. Vanderwerp, W. Lozowski, K. Komisarcik and R.N. Yoder at IUCF and P. Pile, H. Brown, W. McGahern, J. Scaduto, L. Toler, J. Bunce, J. Gould, R. Hackenburg and C. Woody at AGS for their assistance with these experiments. This work was supported by the U.S. Department of Energy and National Science Foundation, the National Sciences and Engineering Research Council of Canada, Grant No. P03B 048 15 of the Polish State Committee for Scientific Research, Indiana University Office of Research and the University Graduate School, Simon Fraser University and the Robert A. Welch Foundation.

References

[1] Multifragmentation, Proc. of the XXVII Int. Workshop on Gross Properties of Nuclei and Nuclear Excitations (Ed. H. Feldmeyer, J. Knoll, W. Nörenberg and J. Wambach, GSi, Darmstadt, Germany) 1999, ISSN 0720-8715.

[2] J. Pochodzalla *et al.*, Phys. Rev. Lett. **75** (1995) 1040.

[3] F. Goldenbaum *et al.*, Phys. Rev. Lett. **77** (1996) 1230; L. Pienkowski *et al.*, Phys. Lett B**336** (1994) 147.

[4] K. Kwiatkowski *et al.*, Phys. Lett. B**423** (1998) 21.

[5] K.B. Morley *et al.*, Phys. Rev. C**54**, 737 (1996).

[6] J. Cugnon, *et al.*, Nucl. Phys. **A470** (1987) 558, Phys. of At. Nucl. **57** (1994) 1075.

[7] G. Wang, K. Kwiatkowski, V.E. Viola, W. Bauer and P. Danielewicz, Phys. Rev. C.**53** (1996) 1811.

[8] J.P. Bondorf, A.S. Botvina, A.S. Iljinov, I.N. Mishustin and K. Sneppen, Phys. Rep. **257** 1995) 133; A. Botvina, A.S. Iljinov and I.N. Mishustin, Nucl. Phys. **A507** (1990) 649.

[9] W.A. Friedman, Phys. Rev. C**42** (1990) 667.

[10] D. H. E. Gross, Rep. Prog. Phys. 53 (1990) 605.

[11] V. Toneev, N.S. Amelin, K.K. Gudima and S. Yu. Sivoklokov, Nucl. Phys. **A519** (1990) 463c.

[12] W.-c. Hsi et al., Phys. Rev. Lett. **79** (1997) 817.

[13] N.T. Porile *et al.*, Phys. Rev. C**39** (1989) 1914.

[14] D. Strottman and W.R. Gibbs, Phys. Lett B**149** (1984) 288.

[15] K. Kwiatkowski *et al.*, Nucl. Instr. Meth. A **360** (1995) 571.

[16] T. Lefort *et al.*, submitted to Phys. Rev. Lett.

[17] J.C. Steckmeyer *et al.*, Nucl. Phys. **A500** (1989) 372.

[18] Y.G. Ma *et al.*, Phys. Lett. B**390** (1997) 41.

[19] L. Beaulieu *et al.* in *Proceedings of the Winter Workshop on Nuclear Dynamics*, Park City, UT, 1999. Ed. W. Bauer and G.D. Westfall, to be published.

[20] J.A. Hauger *et al.*, Phys. Rev. Lett.**77** (1996) 235; J.A. Hauger *et al.*, Phys. Rev. C**57** (1998) 764.

[21] J. Toke *et al.*, Phys. Rev. Lett.**75** (1995) 2920.

[22] D. Durand, Nucl. Phys. **A541** (1992) 266, and Code SIMON in preparation.

[23] E. Renshaw Foxford *et al.*, Phys. Rev. C**54** (1991) 749.

[24] F. Goldenbaum *et al.*, Proc. of the Int. Workshop XXVII on Gross Properties of Nuclei and Nuclear Excitations: Multifragmentation, Ed. H. Feldmeier, J. Knoll, W. Nörenberg and J. Wambach (GSI ISSN 0720-8715) (1999) 104.

[25] L. Beaulieu *et al.*, Phys. Rev. C**54** (1996) R973.

[26] A. Schüttauf *et al.*, Nucl. Phys. **A607** (1996) 457.

Fig. 1. Intranuclear cascade predictions [11] of the average excitation energy for events with E* > 50 MeV are shown as a function of momentum for p, π^- and $\bar{p}$ beams incident on ^{197}Au. Inset compares the excitation energy probability distributions for 8 GeV/c π^- and $\bar{p}$ beams

Fig. 2. Excitation energy (left frame) and residue mass probability (right frame) for several of the systems studied in this work, as indicated on figure.

Fig. 3. Bottom: the probability for observing events with excitation energy greater than E* $\geq$ 400 MeV relative to the probability for events with E* = 400 MeV. Systems are indicated on figure. Top: average mass loss ΔA in the fast cascade as a function of excitation energy. Systems are defined in bottom frame.

Fig. 4. Probability distributions for data in Fig. 2, plotted as a function of E*/A of the residue. Systems are defined on figure.

Fig. 5. Top: average ratio of observed and geometry corrected IMFs per residue nucleon as a function of E*/A; symbols are defined in bottom frame. Bottom: power-law parameters τ from fits to the charge distributions as a function of E*/A of the residue. Systems are defined on figure.

Table 1
Ratio of the integrated events beyond multifragmentation threshold to total events with $E^* > 400$ MeV ($E^*/A > 2$ MeV).

beam	p(GeV/c)	T(GeV)	$\frac{P(E^*>800MeV)}{P(E^*>400MeV)}$	$\frac{P(E^*>1000MeV)}{P(E^*>400MeV)}$	$\frac{P(E^*/A>5MeV)}{P(E^*/A>2MeV)}$
E900a $\bar{p}$	8.0	7.2	0.30	0.097	0.27
E900 p	14.6	13.7	0.23	0.067	0.21
E900 p	12.8	11.9	0.25	0.076	0.22
E900 p	10.2	9.3	0.23	0.066	0.19
E900 π^-	9.2	9.1	0.21	0.058	0.17
E900a π^-	8.0	7.9	0.21	0.056	0.18
E900 π^-	8.2	8.1	0.20	0.054	0.17
E900 p	6.2	5.3	0.19	0.045	0.13
E900 π^-	5.0	4.9	0.17	0.036	0.11
^{3}He [10]	7.6	4.8	0.12	0.020	N/A
$\bar{p}$ [8]	2.1	1.2	0.042	0.003	N/A

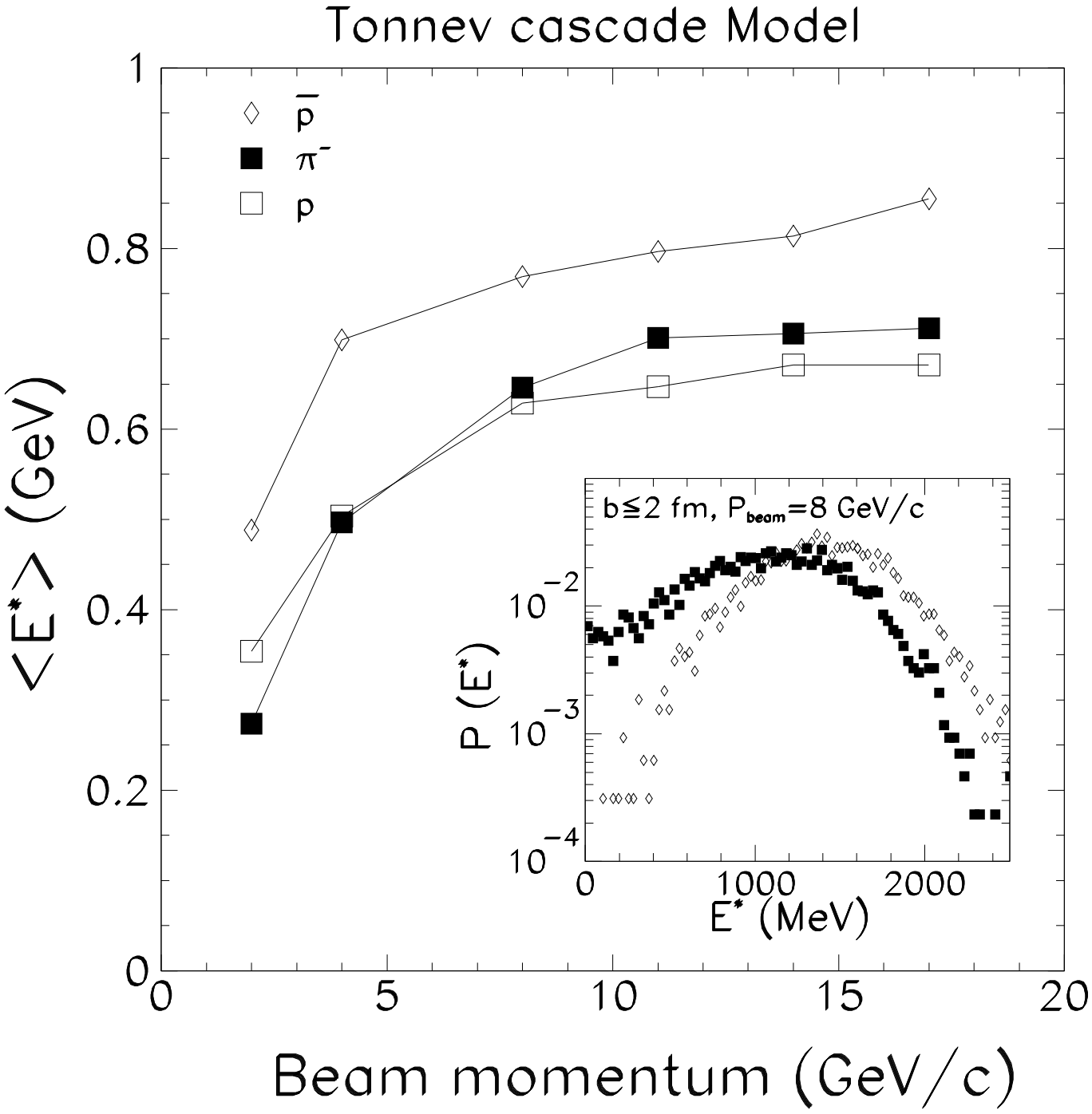

Fig. 1: L. Beaulieu *et al.*

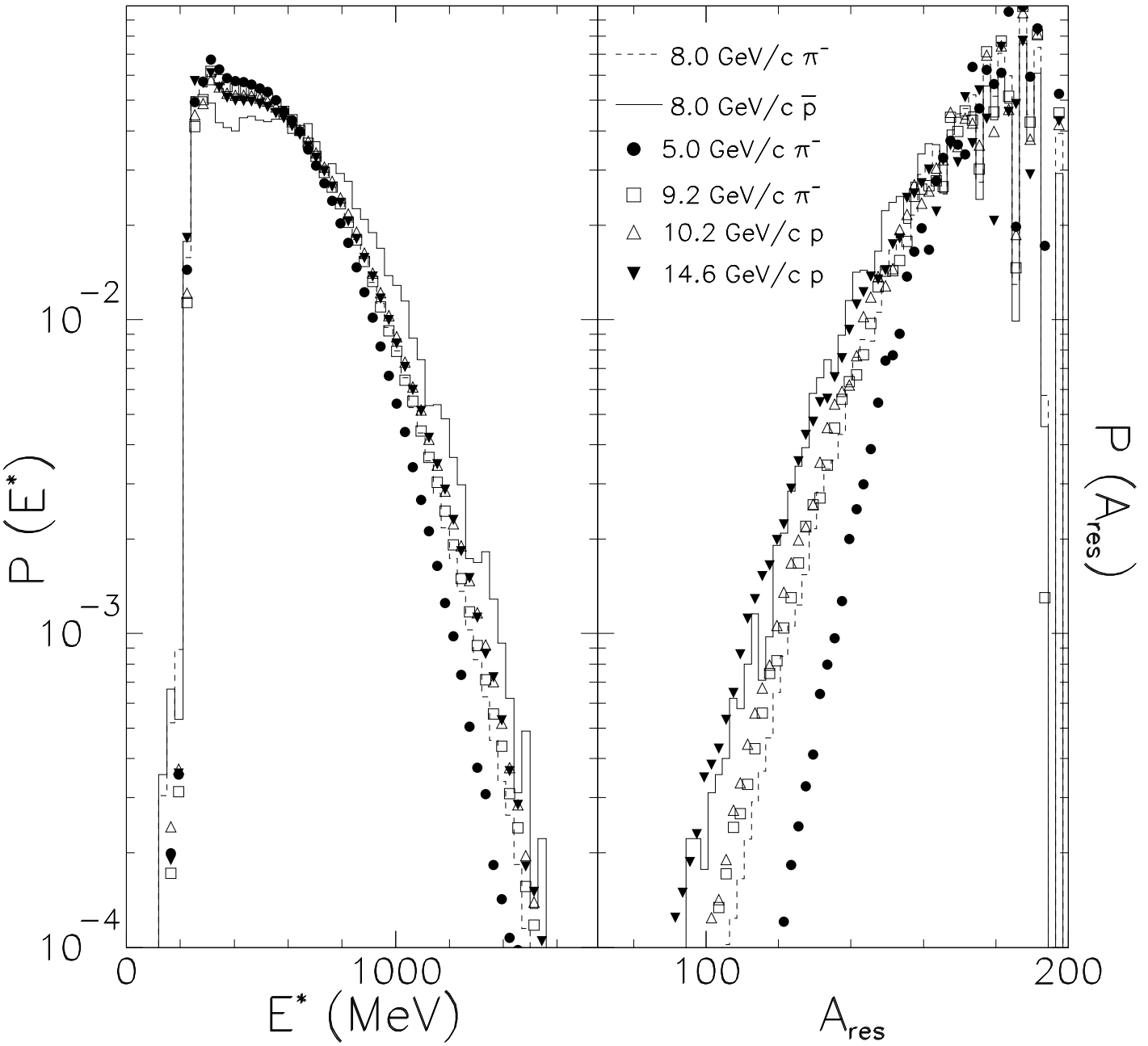

Fig. 2.: L. Beaulieu *et al.*

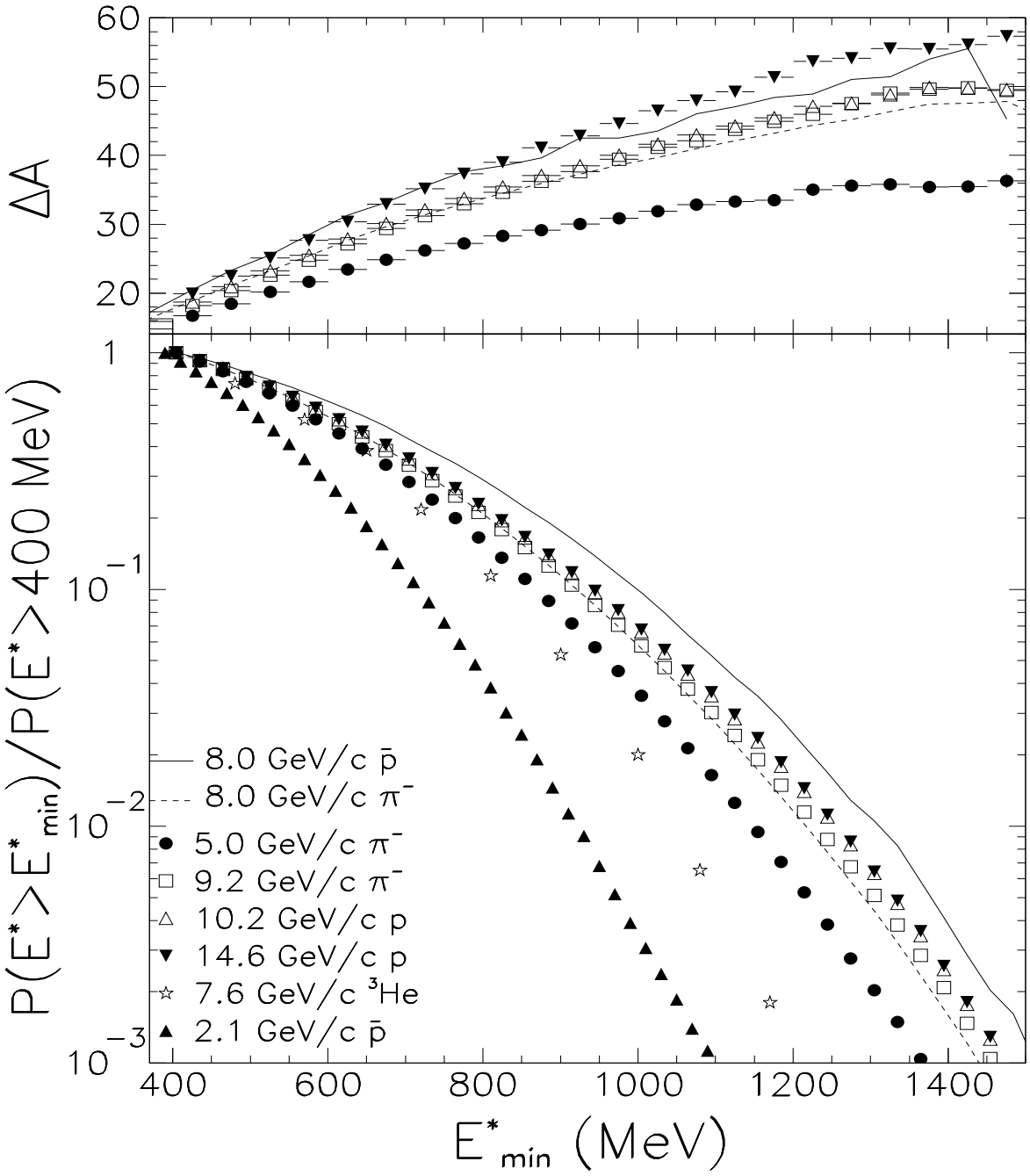

Fig. 3: L. Beaulieu *et al.*

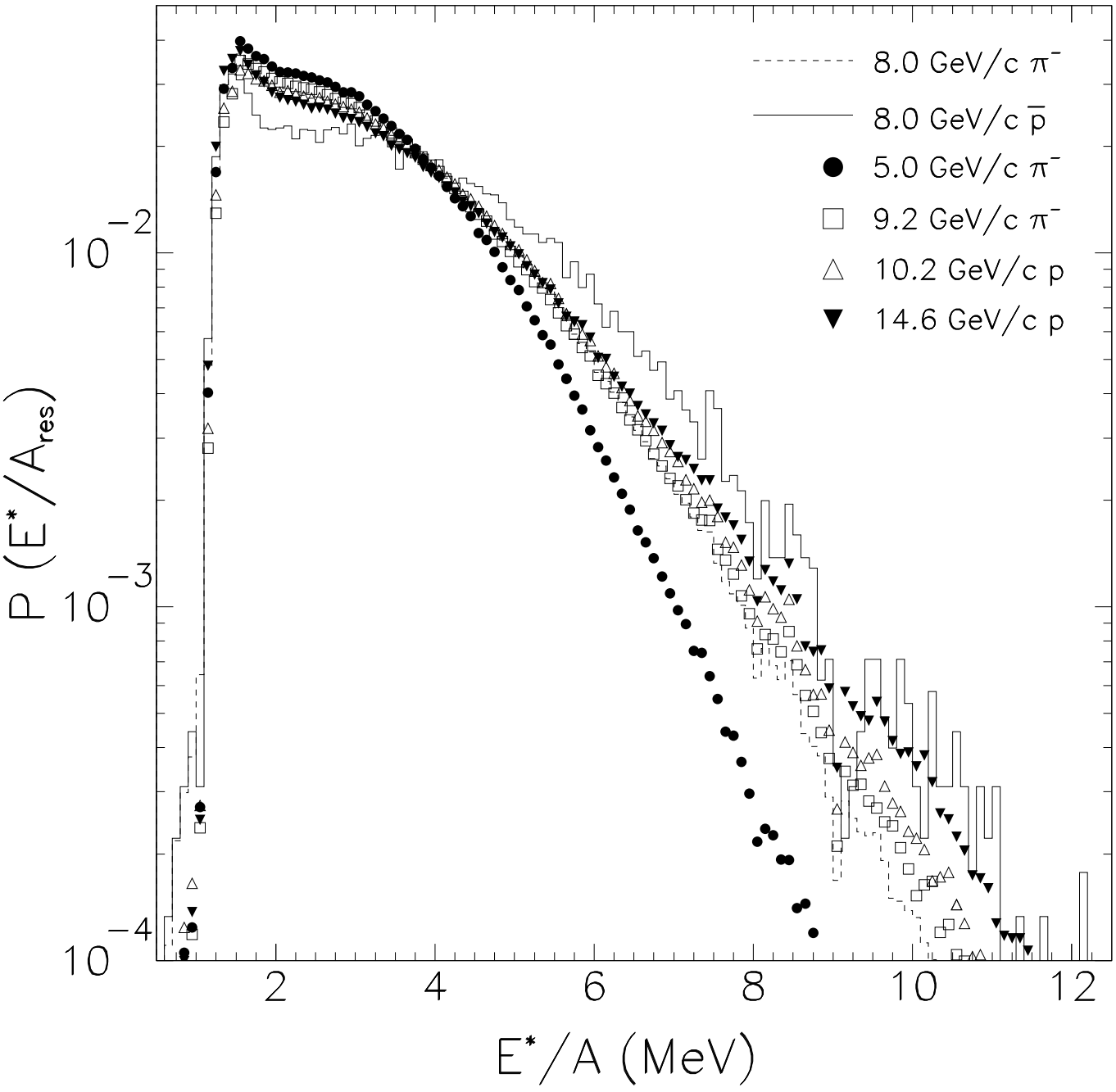

Fig. 4.: L. Beaulieu *et al.*

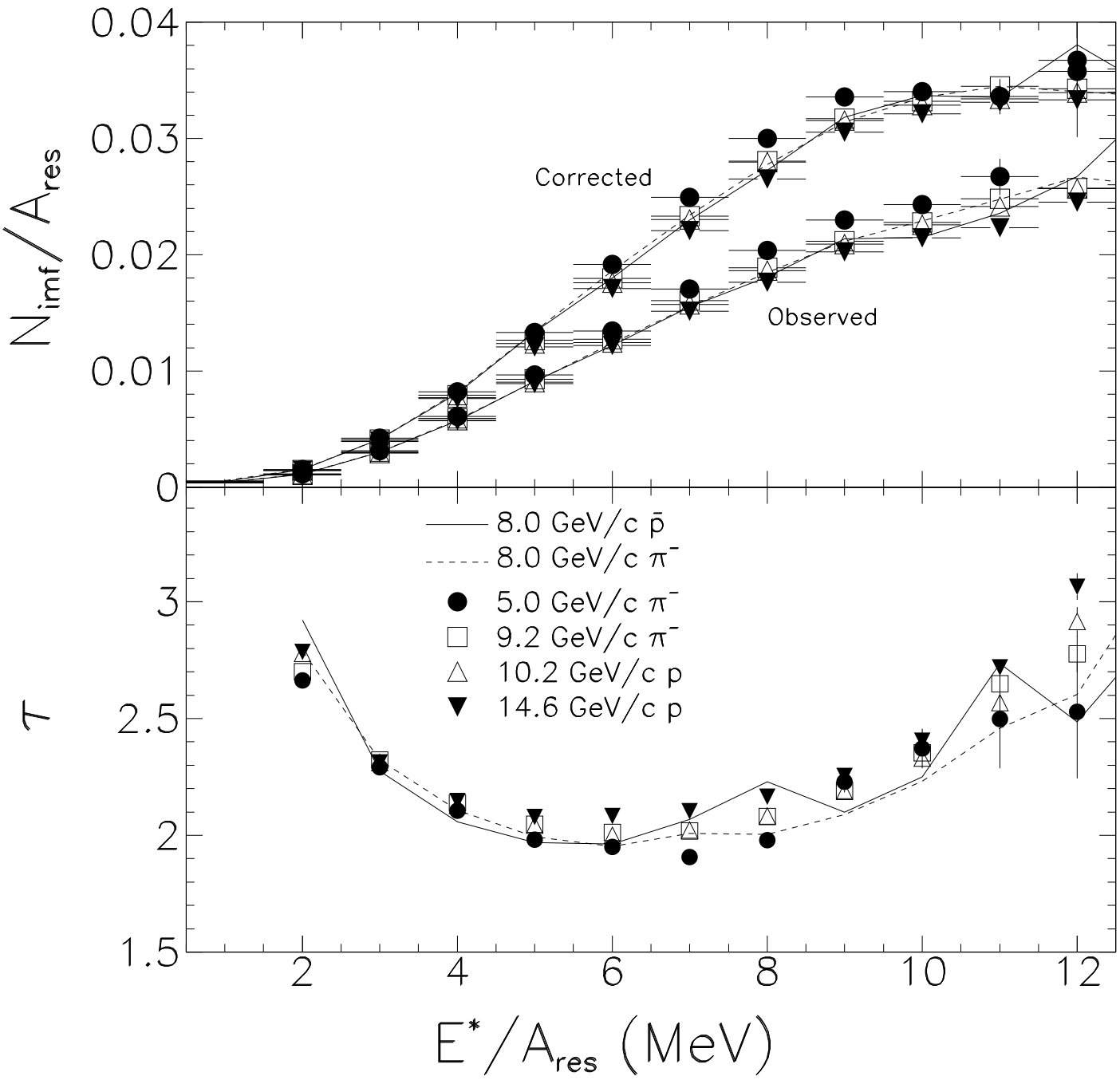

Fig. 5.: L. Beaulieu *et al.*